Biological Conservation 291 (2024) 110474

Contents lists available at ScienceDirect

Biological Conservation

journal homepage: www.elsevier.com/locate/biocon

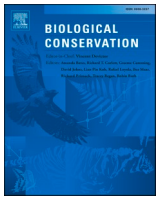

Does size matter? Investigation of the effect of wind turbine size on bird and bat mortality

Julie C. Garvin [a,*], Juniper L. Simonis [b], Jennifer L. Taylor [a]

[a] Tetra Tech, Inc., 1750 S Harbor Way, Suite 400, Portland, OR 97201, USA
[b] DAPPER Stats, 3519 NE 15th Ave, Suite 467, Portland, OR 97212, USA

ARTICLE INFO

Keywords:
Wind energy
Theoretical framework
Blade length
Collision
Fatality estimation

ABSTRACT

Advancements in wind turbine technology have led to larger, more energy productive turbines. However, the degree to which increases in turbine size may affect wildlife mortality is not yet understood. We developed a Bayesian hierarchical model to investigate the potential influence of three turbine size parameters (ground clearance, rotor diameter, and power rating) on fatality rates and fall distances of three representative species: hoary bat (*Lasiurus cinereus*), horned lark (*Eremophila alpestris*), and red-tailed hawk (*Buteo jamaicensis*). Our model incorporated a paired design to isolate turbine size effects, assuming turbines monitored in the same year and in close proximity were similarly influenced by random effects such as weather and habitat. We used Integrated Population Integral Projection Modeling to analyze four component datasets (searcher efficiency, carcass persistence, fatality rates, and fall distributions) derived from focal and priors datasets. Our model showed generally consistent and well-mixed results despite its size and complexity. Decreasing ground clearance led to increased fatality rates for all three species and was most pronounced for hoary bats; increased rotor diameter led to increased fatality rates for red-tailed hawks and for horned larks to a lesser extent. Increasing power capacity led to increased horned lark fatality rates, with a weaker influence on red-tailed hawks. Turbine size covariates had strong species-specific effects on fall distributions with implications for selecting search plot dimensions and analyzing fatality estimates in future studies. To our knowledge, this is the first investigation of ground-clearance effects on fatality rates and of turbine size parameters on carcass fall distributions.

1. Introduction

Advancements in wind turbine technology have led to larger, more energy productive and efficient turbines being installed in new onshore and offshore facilities and used to retrofit existing facilities (Loss et al., 2013; Lacal-Arántegui et al., 2020; Huso et al., 2021). The need to understand the relationship between turbine size and wildlife mortality is pressing, as the ongoing optimization of power production and engineering drives industry toward larger turbine dimensions (LaNier, 2005; Lantz et al., 2019) and climate change concerns lead to increased need and demand for renewable energy (U.S. Department of Energy, 2019; Huso et al., 2021). The degree to which increases in turbine size affect bird and bat mortality influences both wind project development and wildlife management decisions, with project- and species-specific consequences (Barclay et al., 2007; AWWI, 2017; Anderson et al., 2022). Previous investigations into the impact of turbine size on wildlife mortality have found a variety of relationships among taxa – including positive, negative, and equivocal – both within and among meta-analyses (Barclay et al., 2007; Loss et al., 2013; Smallwood, 2013). Such highly context-specific results speak to the current challenge in providing conclusive answers to questions about the influence of turbine size on wildlife mortality. Furthermore, the wide variety of analytical methods used in these studies speaks to the need for generalized and flexible statistical models to combine the variety of data collected and discern the most influential relationships for operational decision making.

The relationship between turbine size and wildlife mortality is muddied at least in part because "size" is a catch-all term used interchangeably for multiple correlated measurements. The size parameter most commonly used in analyses of turbine size is hub height, although power capacity rating is also used (Barclay et al., 2007; Loss et al., 2013; Smallwood, 2013; Huso et al., 2021), despite not being a measure of geometric size, per se. Hub height sets the location of the rotor-swept zone in airspace, but does not directly influence the size of the rotor-

* Corresponding author.
E-mail addresses: julesgarvin@hotmail.com (J.C. Garvin), simonis@dapperstats.com (J.L. Simonis), Jennifer.Taylor@tetratech.com (J.L. Taylor).

https://doi.org/10.1016/j.biocon.2024.110474
Received 20 July 2023; Received in revised form 22 December 2023; Accepted 22 January 2024
Available online 13 February 2024

swept zone. Although these geometric specifications as well as facility operations (e.g., downtime) have the potential to inform the relationship between size and wildlife mortality (Huso et al., 2021; Prakash and Markfort, 2021), many are rarely reported publicly, hindering their inclusion in analyses (Nicholson, 2011; Sassi, 2016). Further complicating the relationship between turbine size and mortality are the variety of covariates that dictate the wildlife-turbine interaction, including the rotor speed and pitch of the blade (Tucker, 1996; Band et al., 2007); body size, flight behavior, visual acuity, and other aspects of the wildlife species or group of interest (Smales et al., 2013; Khosravifard et al., 2020); environmental variables such as land cover, wind speed and prey availability (Baerwald et al., 2009; Cryan et al., 2014; Thompson et al., 2017); and temporal drivers such as time of day and season (de Lucas et al., 2008; Krijgsveld et al., 2009).

Because estimating turbine-level effects is not currently feasible with existing fatality estimation tools, we use a custom Bayesian hierarchical model in our study to capture the potential influence of turbine size on North American fatality rates. Currently available estimators like Evidence of Absence (Dalthorp et al., 2017) and GenEst (Dalthorp et al., 2018) do not allow for turbine covariates and/or assume that no turbines have 0 carcasses. In contrast, a Bayesian-based estimator can address these challenges while handling an open population with imperfect detection, unknown size, and unknown detection rates (Hobbs and Hooten, 2015). We address these challenges via three mechanisms: [1] our integrated modeling approach that incorporates independent estimates of "vital rates" via searcher efficiency and carcass persistence trials (Zipkin et al., 2014); [2] inclusion of hierarchical "random effects" and covariate-based "fixed effects" into the vital rate models (Sólymos et al., 2012); and [3] information sharing via a Bayesian hierarchical connection among carcass population observations via a common arrival (i.e., fatality) rate equation (Hobbs and Hooten, 2015). Leveraging a Bayesian paradigm, we incorporate prior data regarding all model components – searcher efficiency, carcass persistence, species-specific fatality rates, and fall distributions – available in existing publications (Appendix S1).

We apply this model to post-construction mortality (PCM) data extracted from U.S. and Canadian databases. The sampling schemas defining these observations of fatalities vary spatiotemporally (e.g., circular vs. "road and pad" plot; Maurer et al., 2020), and the data recorded on surveys (number of carcasses) are discretely distributed, highly 0-inflated, overdispersed, and spatiotemporally autocorrelated. Therefore, we estimated turbine-level fatality rates, accounting for site-level variation which can heavily influence estimates of mortality (Erickson et al., 2014; Marques et al., 2014; Hobbs and Hooten, 2015). We use a paired design to facilitate our estimation of turbine size effect and assume turbines in relatively close proximity experience similar densities and movement patterns of wildlife. We therefore constrained our analysis to PCM data derived from turbine *mosaics*. Projects that incorporated more than one turbine size were categorized as *in-project mosaics* whereas data from two or more adjacent projects with different turbine sizes that were monitored in the same year using comparable protocols were categorized as *neighbor mosaics* (Appendix S2). These turbine-mosaics facilitate testing the effect of turbine size on fatality rates while controlling for site-specific factors that influence fatality rates (e.g., habitat, local bird or bat community, geographic region) including those for which data are not typically available (e.g., wind regime, bird and bat exposure rates).

2. Methods

2.1. Dataset

We identified 175 candidate mosaic projects from the American Wind and Wildlife Information Center (AWWIC) database, the [Canadian] Wind Energy Bird and Bat Monitoring Database (WEBBMD), publicly available reports, and projects for which Tetra Tech was provided data by cooperating wind companies for the purpose of this research. Our selection criteria were designed to identify in-project and neighbor mosaics that used utility-scale wind turbines (e.g., 1 megawatt [MW] or larger), performed PCM with statistical methods that meet current industry standards, and for which sufficient data were available for analysis (complete set of criteria provided in Appendix S2). Note that project inclusion was independent of occurrence of fatalities of our focal species (defined below). A project with zero fatalities detected of a species of interest is a valid datapoint when analyzing mortality correlates because potential outcomes include zero fatalities. Furthermore, fatality estimates in regions where a species is absent (e.g., Hawaii) provide an additional mechanism for model validation.

Ninety-one mosaic projects (in-project mosaics and members of neighbor mosaics) met our project selection criteria. Although the AWWIC database alone contains >340 studies (AWWI, 2020a; AWWI, 2020b), only a small proportion had raw data suitable for analysis. Forty-four of these projects hosted 88 PCM studies between 2007 and 2019 that met our data selection criteria and were carried forward for analysis. These 44 projects represented 24 mosaics, 15 were in-project mosaics and nine were neighbor mosaics. Bird Conservation Regions (BCR; Bird Studies Canada and NABCI, 2014) were used to represent ecologically distinct regions within North America to capture geographic variation among mosaics. The 44 projects included for analysis were distributed among 12 BCRs, with 27 projects clustered within the Lower Great Lakes/St. Lawrence Plain (BCR 13); the majority of BCRs contain one or two projects (Fig. 1).

Each of the 88 studies represented a maximum of one year time window which was segmented into seasons. These studies had between 6 and 368 turbines that were searched per focal project (Fig. 2). Turbines were searched at scheduled intervals of between 3.5 and 34 d. The turbines present at these sites ($N = 1630$) varied widely among size parameters. Hub height ranged from 55 to 110 m and rotor diameter ranged from 61 to 136 m, producing ground clearances (hub height − half-rotor diameter) between 20 and 54 m and maximum blade-tip height (MBTH; hub height + half-rotor diameter) from 90 to 173 m. Power ratings ($N = 23$) ranged between 1.0 and 3.6 MW, with a mean power rating per turbine of 1.91 MW (± 0.5). Given the known correlation among multiple turbine size metrics, we limited our analysis to three turbine parameters. Power rating was selected to address the focal need to minimize wildlife impacts while maximizing energy production; ground clearance was included because it defines the space below sweeping blades where resident birds frequently fly (Wulff et al., 2016); and rotor diameter was chosen to represent the extent of the turbine's rotor-swept zone (correlation among turbine-level values: power and ground clearance = −0.053, power and rotor diameter = 0.823, ground clearance and rotor diameter = −0.285).

Turbine size appears to influence taxa differentially (Loss et al., 2013; Smallwood, 2013; Zimmerling and Francis, 2016; Thompson et al., 2017; Anderson et al., 2022). We therefore apply our model to species representative of taxonomic groups of conservation concern relative to wind-wildlife interactions (Arnett and Baerwald, 2013; Watson et al., 2018): bats, raptors, and grassland songbirds. We selected a species from each group that was commonly detected as carcasses (i.e., sufficient sample size for robust analyses) and broadly distributed geographically: hoary bat (*Lasiurus cinereus*; $N = 1633$ [excludes the Hawaiian hoary bat, *Lasiurus semotus*]), horned lark (*Eremophila alpestris*; $N = 309$), and red-tailed hawk (*Buteo jamaicensis*; $N = 60$).

The dataset we developed to inform our model's priors was curated from publicly available PCM reports and published literature (Appendix S1). Data sources had to meet similar selection criteria as our focal dataset (Appendix S2), although they were not limited to in-project or neighbor mosaic facilities. Summary-level data (i.e., point estimates with standard errors or confidence intervals) were incorporated for the searcher efficiency, carcass persistence and arrival rate components of the model, whereas raw data on carcass fall distributions were used for the fall distribution component. Data were derived from an additional

Fig. 1. Distribution of focal datasets among Bird Conservation Regions (BCR) in the U.S. and Canada.

59 sources – comprising 252 projects from 166 mosaics – that were not present in our focal dataset (Appendix S2). These projects were from 20 BCRs, including 8 of the 12 focal regions as well as an additional 12 BCRs not present in the focal dataset.

2.2. Statistical analysis

2.2.1. Modeling approach

We analyze the component datasets (searcher efficiency [ψ], carcass persistence [ρ], arrival rates [α], and fall distributions [f]) using Integrated Population Integral Projection Modeling (IPIPM; Schaub and Abadi, 2011; Plard et al., 2019), which takes a multi-data view of populations structured via continuous traits. We treat carcasses as existing within populations of dead animals where their traits—specifically, location and age—influence how they persist ("survive" in the population of carcasses) and are detected over time. Following standards for carcass studies in which an observed carcass may only be counted once, we model the population as being subjected to removal sampling (Wyatt, 2002) in addition to actual carcass loss, and loss to decomposition and scavengers. The combination of removal sampling with an open population presents identifiability issues under observation-only datasets—it is not clear if an unobserved carcass is present but not seen or not present (Cooch and White, 2002). Hundreds of wind energy mortality studies conducted to date have quantified carcass arrival date, location, carcass persistence, and searcher efficiency using experimental and observational data collected across spatiotemporal scales (Appendix S1). The use of an integrated Bayesian paradigm facilitates information sharing among our focal data and prior studies (Appendix S1), efficient analysis of highly unbalanced hierarchical data (Hobbs and Hooten, 2015), and mitigation of identifiability constraints of a classic open population under removal sampling (Dail and Madsen, 2011).

We use a multinomial-Poisson N-mixture distribution to represent the statistical processes of carcass arrival and detection based on composites of basal parameters (Royle, 2004; Haines, 2016; Haines, 2020). The multinomial observation model allows us to explicitly incorporate removal sampling and distance sampling and is supported by prior application to rare wildlife populations (Wyatt, 2002; Chandler et al., 2011; Sollmann et al., 2015). The Poisson distribution defines the total arrivals of carcasses to each plot, and the random-effects approach detailed below facilitates incorporation of overdispersion without requiring the use of the more computationally expensive negative binomial distribution (Haines, 2020).

2.2.2. Terms and functions

A *search* is conducted on a *day* at a *plot*, which is the space surrounding a *turbine* at a *project* within a *mosaic* from a *region*, observed for a defined study duration. The area of each plot searched is allocated among a standardized set of 15 10-m wide concentric *bands*.

The vector of counts of carcasses observed in plot i over J_i searches, $\boldsymbol{y}_i$, follows a multinomial-binomial-Poisson distribution with mean total carcasses κ_i, density-weighted probability of landing within searched area δ_i, and search-specific detection probabilities $\boldsymbol{\pi}_i$:

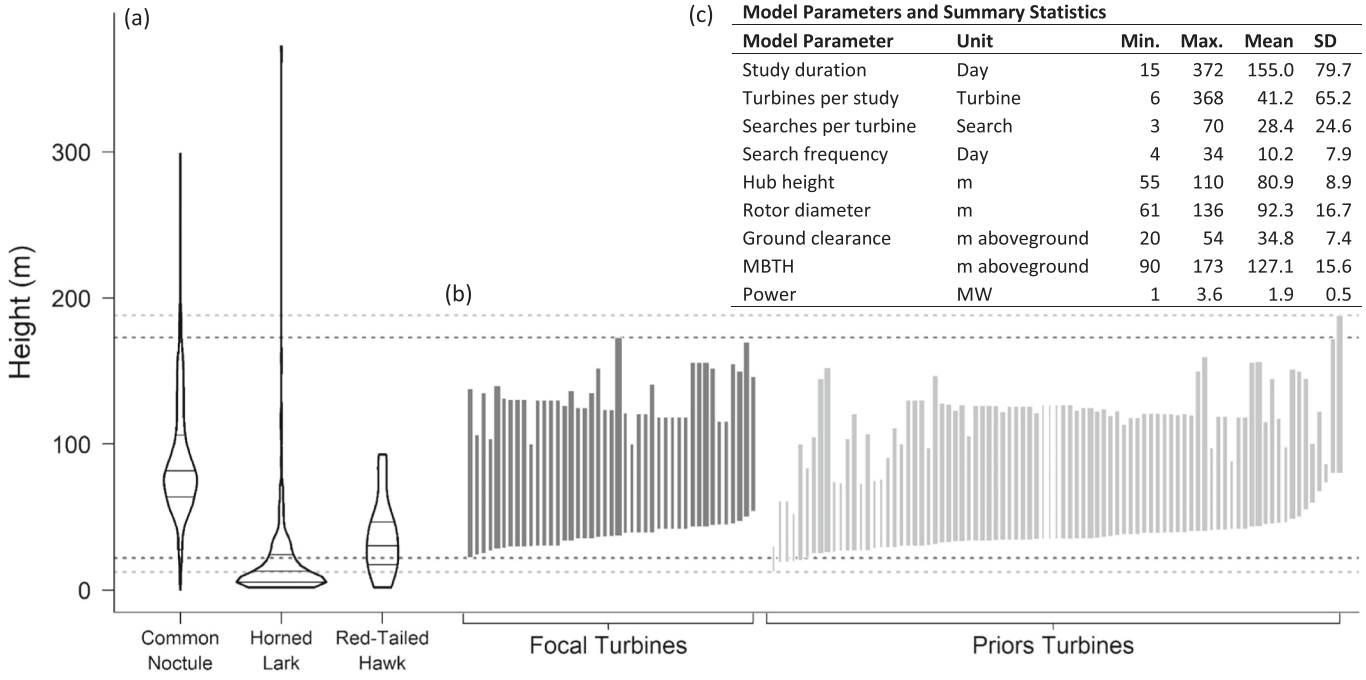

(c) **Model Parameters and Summary Statistics**

Model Parameter	Unit	Min.	Max.	Mean	SD
Study duration	Day	15	372	155.0	79.7
Turbines per study	Turbine	6	368	41.2	65.2
Searches per turbine	Search	3	70	28.4	24.6
Search frequency	Day	4	34	10.2	7.9
Hub height	m	55	110	80.9	8.9
Rotor diameter	m	61	136	92.3	16.7
Ground clearance	m aboveground	20	54	34.8	7.4
MBTH	m aboveground	90	173	127.1	15.6
Power	MW	1	3.6	1.9	0.5

Fig. 2. (a) Flight heights of representative species aboveground (common noctule [*Nyctalus noctula*] values presented from Roeleke et al. [2016] as a proxy for hoary bat given dearth of published hoary bat flight heights; horned lark and red-tailed hawk flight heights from Wulff et al. (2016)) (b) Ground clearance (space below), rotor diameter, maximum blade-tip height (tallest point), and power rating (indicated by line weight) of focal and priors turbines in analysis dataset, (c) Summary statistics of model parameters and turbine size metrics.

$$\boldsymbol{y}_i \sim mbP(\kappa_i, \delta_i, \boldsymbol{\pi}_i)$$

where the arrival total is the sum of the day-level daily arrival rates (i.e., fatality rates, converted from day-level yearly arrival rates):

$$\kappa_i = \sum_{d=1}^{D_i} \alpha_i / 365$$

The probability a carcass lands in any searched area across the plot is the summed density weighted proportion of area searched across the bands. The contribution for each band is the product of the fraction of the fall distribution ($f(\varphi_i)$) within the band (from inner radius $r0$ to outer radius $r1$) and the percentage of the area within the band that is searched:

$$\delta_i = \sum_{b=1}^{15} \left(\int_{r0_b}^{r1_b} f(\varphi_i) \right) a_{ib}$$

The probability of a carcass being observed on a specific search π_{ij} is the sum of daily contributions for each day from the start of its arrival to the plot to the day of the search d_j. A carcass that arrives on day d must survive by persisting through each day from d to d_j according to the order of arrival, persistence, and search (if there is a search that day):

$$\pi_{ij} = \sum_{d=1}^{d_j} \left(\alpha_d \Big/ \sum \alpha_d \prod_{k=d}^{d_j} \rho_k \prod_{k=d}^{d_j-1} (1 - \psi_k) \right)$$

where $\frac{\alpha_d}{\sum \alpha_d}$ is the proportion of total plot-level arrival that occurs on d and $\psi_k = 0$ on non-search days. The probability that a carcass that has landed in the searched area of plot i is ever observed (aka, $\hat{g}$) is then the sum of search-level detection probabilities:

$$\pi_i = \sum_{j=1}^{J_i} \pi_{ij}$$

The field trial and prior data are then integrated with the focal carcass searches via shared process parameters.

We modeled logit-scale searcher efficiency ψ and carcass persistence ρ as linear models with intercept, region, and mosaic effects associated with the plot and season effect based on the day.

$$\text{logit}\psi_{id} = \psi_0 + \gamma^{\psi}_{region_i} + \gamma^{\psi}_{mosaic_i} + \gamma^{\psi}_{season_d}$$

$$\text{logit}\rho_{id} = \rho_0 + \gamma^{\rho}_{region_i} + \gamma^{\rho}_{mosaic_i} + \gamma^{\rho}_{season_d}$$

The fall distance for a carcass in a plot is a log-linear function of an overall intercept and fixed effects for ground clearance, rotor diameter, and power rating associated with the turbine of the plot.

$$log\varphi_i = \varphi_0 + x^{\varphi}_{gc_i}\beta^{\varphi}_{gc_i} + x^{\varphi}_{rd_i}\beta^{\varphi}_{rd_i} + x^{\varphi}_{mw_i}\beta^{\varphi}_{mw_i}$$

We modeled log-scale annual arrival rate as a linear model of an overall intercept; fixed effects for ground clearance, rotor diameter, and power turbine covariates; and region and mosaic random effects associated with the plot.

$$log\alpha_i = \alpha_0 + x^{\alpha}_{gc_i}\beta^{\alpha}_{gc_i} + x^{\alpha}_{rd_i}\beta^{\alpha}_{rd_i} + x^{\alpha}_{mw_i}\beta^{\alpha}_{mw_i} + \gamma^{\alpha}_{region_i} + \gamma^{\alpha}_{mosaic_i}$$

The priors data for arrival were reported as rates (w^{α}_p for prior study p), which we log-transformed and fit using a normal observation model with means $log\alpha_p$ based on the region and mosaic of the study; an overall intercept; and fixed effects for ground clearance, rotor diameter, and power rating. We included the reported sample standard deviations σ^{α}_p weighted by relative log-sample sizes N^{α}_p (divided by mean log sample size $\overline{logN^{\alpha}}$).

$$w^{\alpha}_p \sim N\left(log\alpha_p, \sigma^{\alpha}_p \left(logN^{\alpha}_p \Big/ \overline{logN^{\alpha}} \right)^{-1/2} \right)$$

The priors data for both searcher efficiency and carcass persistence were reported as rates (w^{ψ}_p, w^{ρ}_p), which we logit-transformed and fit using normal observation models with means $\text{logit}\psi_p$ and $\text{logit}\rho_p$ based on the region, mosaic, and season of the study and reported sample standard

deviations

σ_p^{ψ}, σ_p^{ρ} weighted by relative log-sample sizes N_p^{ψ}, N_p^{ρ} (divided by mean log sample sizes $\overline{logN^{\psi}}$, $\overline{logN^{\rho}}$).

$$w_p^{\psi} \sim N\left(\text{logit}\psi_p, \sigma_p^{\psi}\left(logN_p^{\psi}\Big/\overline{logN^{\psi}}\right)^{-1/2}\right)$$

$$w_p^{\rho} \sim N\left(\text{logit}\rho_p, \sigma_p^{\rho}\left(logN_p^{\rho}\Big/\overline{logN^{\rho}}\right)^{-1/2}\right)$$

The searcher efficiency trials data were reported as success or failure (w_t^{ψ} for trial t), which we modeled as Bernoulli observations with detection probability ψ_t

$$w_t^{\psi} \sim Bern(\psi_t)$$

The carcass persistence trials data were reported as presence-absence on successive searches ($\boldsymbol{w}_t^{\rho}$ for trial t), which we modeled as a joint interval-exponential distribution with time to removal $\frac{1}{1-\rho_t}$ and cut-points based on search days $\boldsymbol{c}_t$

$$\boldsymbol{w}_t^{\rho} \sim iexp(1-\rho_t, \boldsymbol{c}_t)$$

Given that carcass fall distances (z_i) are measured on observations only after they are found (i.e., there are no trials), we incorporate the proportion of area searched in all analyses to account for carcasses that fell outside the searched areas. Recognizing the propensity for non-normal skew and kurtosis in carcass fall distributions, we used a generalized non-standard t distribution to model the continuous response of carcass distance (Kruschke, 2015) with mean, scale, and degrees of freedom

$$f(\varphi_i) \sim t(\varphi_i, \varsigma, \nu)$$

To align the fall distribution with carcass observations and the proportion area searched, we integrated the fall distribution ($f(\varphi_i)$) at 10-m intervals from 0 to 150 m and multiply each band by its proportion of area searched.

The carcasses with distances measured (m_i) are then distributed among the distance bands via a multinomial distribution with probabilities corresponding to the relative density weighted proportion in each band ($\dot{\delta}_{ib}$ where the dot accent indicates relative)

$$\dot{\delta}_{ib} = \frac{\delta_{ib}}{\delta_i} = \frac{\left(\int_{r0_b}^{r1_b} f(\varphi_i)\right) a_{ib}}{\sum_{b=1}^{15}\left(\int_{r0_b}^{r1_b} f(\varphi_i)\right) a_{ib}}$$

$$z_i \sim multi\left(m_i, \dot{\boldsymbol{\delta}}_i\right)$$

This same approach was used separately for the priors and trials datasets.

Hyper-priors used to define the shared parameters were chosen to generate weakly informative prior distributions (Appendix S1). Intercept and fixed effects parameters were modeled with normal distributions with means centered on the observed values and parameter-specific variances. We modeled the random effects standard deviations and the scale parameter for the fall distribution using uniform distributions. We used an exponential distribution to model the degrees of freedom parameter for the fall distribution model.

2.2.3. Implementation

Models were fit in R 4.2.1 (R Core Team, 2022) using custom code (Appendix S3) and driven by the package nimble – (v. 0.13.0; de Valpine et al., 2017, 2022), with additional tools from nimbleEcology (v. 0.4.1; Goldstein et al., 2021) and coda (v. 0.19-4; Plummer et al., 2006) packages. All parameters were sampled using an adaptive Metropolis-Hasting (random walk) algorithm (Shaby and Wells, 2011), with an initial proposed standard deviation of 1, an adaptation interval of 50 iterations on the linear scale with decay exponent of 0.8, and without reflection. Six chains were run of each model, with different and randomly determined initial parameter values from distributions approximating the priors, for 30,000 iterations each, discarding the first 20,000 as burn-in, leaving the final 10,000 values that we thinned to 1000 for each chain. We evaluated chain convergence using the auto-correlation, effective sample size adjusted for autocorrelation, and partial scale reduction factor (i.e., Gelman-Rubin statistic; Gelman and Rubin, 1992) for each parameter and performed posterior predictive checks with omnibus and targeted strategies (Gelman et al., 2014) to quantify the model's ability to predict data resembling the observations.

We facilitated computational efficiency of this highly complex and large model through custom software (Appendix S3) that substantially expands the core models of EoA (Dalthorp et al., 2017) and GenEst (Dalthorp et al., 2018). Leveraging the extensibility of nimble, we built a custom response distribution and functions to expeditiously calculate core quantities, like $\boldsymbol{\pi}_{1:J_i}$. We used extensive nested indexing with pre-constructed pointer variables to reduce the impacts of the 0-inflated nature of the dataset and minimize calculations. We also constructed a model parallelization function using the functionality of the parallel base package in R 4.2.1 (R Core Team, 2022). To minimize computational demands, we did not track region-, mosaic-, and season-specific random effects estimates, only their standard deviation. The three species' models were run simultaneously through terminal multiplexing with tmux v 3.3a (Marriot, 2022) on a DigitalOcean memory-optimized, dedicated virtual machine ("droplet"; 32 vCPUs, 256 GB Memory) running the Ubuntu 22.04 × 64 image.

3. Results

3.1. Model performance

Our model showed generally consistent and well-mixed results despite its size and complexity, with some important exceptions. Intriguingly, the parameters that suffered from poor mixing were not consistent across the three species. The number of parameters and integrated, hierarchical structure led to increased autocorrelation and a resulting depression of effective sample sizes.

Despite those parameter estimation concerns, the goodness-of-fit predictive tests indicated that the model produced data that generally reflected the observations (Bayesian p-values all between 0.05 and 0.95). The omnibus χ^2 discrepancy function confirmed that the model produced carcass count data that were reflective of the observations for all three species, albeit not without challenges, perhaps to be expected given that we did not track specific random effects estimates.

More targeted checks showed that the model addressed the challenging distribution by underpredicting the mean while overpredicting the median number of carcasses at searches and within plots. For all three species, the model closely matched but slightly overpredicted the observed proportion of plots and searches with 0 carcasses, and similarly slightly underpredicted the proportion of plots and searches with 1 carcass. The hierarchical uncertainty in the model (exacerbated by the lack of tracking specific errors) did produce some extreme (>10) predicted carcass counts. Although such extremes were rarely predicted for all three species, they were higher for hoary bats, pointing to a more leptokurtic prediction. Our model was also able to faithfully recover observed patterns in the carcass fall distributions for all three species, although the truncated sampling distances combined with the farther fall distances for red-tailed hawks and horned larks reduced fit relative to hoary bats (Section 3.3).

3.2. Fatality rates

Each of our turbine size parameters influenced fatality rates in the same general direction among species (with the exception of hoary bat and power rating) but with different magnitudes (Fig. 3, Table 1). Decreasing ground clearance led to increased fatality rates for all three species but was most pronounced for hoary bats (mean effect size = −0.115, 95 % CI = −0.194, −0.039; Fig. 3a). Power rating was the most influential turbine size covariate for horned lark (mean = 0.271, 95 % CI = 0.068, 0.480; Fig. 3b) with a weaker influence on red-tailed hawk with fatality rates increasing with greater MW capacity. Increased rotor diameter led to increased fatality rates for red-tailed hawk in particular (mean = 0.285, 95 % CI = −0.063, 0.634; Fig. 3c), but also increased horned lark fatality rates to a lesser extent. The influence of power rating and rotor diameter was negligible on hoary bat fatality rates as indicated by a mean effect close to zero (Fig. 3a, Table 1).

The random effects of region and mosaic were highly influential on fatality rates of all three species, although mosaic had a relatively weaker effect on red-tailed hawk fatality rates (mean = 0.312, 95 % CI = 0.054, 0.809) compared to its effect on hoary bat (mean = 1.808, 95 % CI = 1.486, 2.200) and horned lark (mean = 1.738, 95 % CI = 1.365, 2.205) fatality rates. Mosaic had a stronger effect on hoary bat fatality rates than region, whereas horned lark fatality rates were affected by these factors to nearly the same degree (Table 1). There was not even a modest correlation between region-level effect estimates among the three species (pair-wise correlations: hoary bat and horned lark = −0.140; hoary bat and red-tailed hawk = −0.096, horned lark and red-tailed hawk = 0.080).

3.3. Fall distributions

Turbine size covariates were inconsistent in their effect on the fall distance of our focal species (Fig. 3; Table 1). For example, ground clearance had a positive effect on the fall distance of horned lark (Fig. 3e) while having a negative effect on that of hoary bat (Fig. 3d) and red-tailed hawk (Fig. 3f). The fall distances of horned larks and red-tailed hawks were positively affected by power rating but negatively affected by rotor diameter at the same time hoary bat fall distributions were hardly affected by either parameter (Table 1).

4. Discussion

The trends revealed by our analysis are consistent with a recent study that found rotor diameter and power rating to be positively correlated with bird fatality rates (Huso et al., 2021), but contradict findings of that same study and others that found these parameters to be positively correlated with bat fatality rates (e.g., Fiedler et al., 2007; Arnett et al., 2008; Huso et al., 2021). To our knowledge, this is the first PCM study to directly analyze ground-clearance effects on fatality rates.

4.1. Predictors of mortality

Our finding that increases in rotor diameter led to higher fatality rates of horned lark, and red-tailed hawk in particular, is not unprecedented (Huso et al., 2021). However, other empirical studies that have examined this turbine-size parameter on bird fatality rates did not detect such an effect (e.g., Barclay et al., 2007; Everaert, 2014; Minderman et al., 2015). It is likely that variation in site-specific fatality rates confounded their ability to detect such an effect. Indeed, fatality rates of our focal species varied widely among regions and mosaics (Table 1). The regional scale parameter likely reflected differences among ecoregions including climate, habitat associations, and relative abundance within a species' range, all of which could influence fatality rates. The influence of mosaic captured more local scale variables such as land use and land cover, wind regime, topography, and state or species-specific PCM study design standards or guidelines. Red-tailed hawk fatality rates were much less influenced by mosaic than by region, perhaps reflecting landscape-scale patterns in abundance and lack of sensitivity to local factors. In contrast, hoary bat and horned lark fatality rates varied widely among regions and mosaics. The effect of region on hoary bat was not surprising, especially given that 82.5 % of our hoary bat fatalities were derived from BCR 13, where PCM studies are prescribed by provincial permit requirements. Nonetheless, the variation among mosaics was even higher than among regions despite unevenly distributed data at the regional scale (Table 1). The spatially hierarchical structure of our Bayesian model allowed it to accommodate such uneven spatial sampling via borrowing strength (Hobbs and Hooten, 2015).

That ground clearance was the strongest predictor of hoary bat fatality rates was surprising, particularly because hoary bats are thought to primarily forage along treetops and at elevations more consistent with the rotor-swept zone than below it (Menzel et al., 2005). In a study by Foo et al. (2017) of bats foraging near turbines, they recorded 2.75 hoary bat calls per night at ground-based acoustic detectors compared to 33.6 calls per night at detectors mounted approximately 85 m above-ground on turbine nacelles. However, recent research indicates that bat activity below the nacelle may be greater than previously thought (Peterson et al., 2022). More studies are needed on hoary bat flight heights to better understand the causal relationship with ground clearance.

The latest trend in turbine technology is to use taller hub heights, typically in conjunction with longer rotor diameters, than previous models (Lantz et al., 2019). In contrast, repowering of existing turbines via blade or nacelle replacement (i.e., turbine modification) without changing the hub height will result in decreased ground clearances. Given the ageing wind fleet in North America and the appealing economics of repowering, our research suggests that widespread turbine modifications have the potential to exacerbate the already worrisome level of hoary bat fatality rates across North America (e.g., Friedenberg and Frick, 2021; EPRI, 2020).

4.2. Implications of fall distributions

The patterns revealed by our model call into question the theory that taller turbines throw a given carcass farther than shorter turbines (e.g., Hull and Muir, 2010). Indeed, ground clearance, our strongest predictor of fall distance, varied independently of MBTH (Fig. 2; correlation among turbine-level values: ground clearance and MBTH = 0.176). As a result, carcasses of a given species were sometimes thrown farther by a shorter turbine and sometimes farther by a taller turbine. The relationship of fall distribution with ground clearance was also highly species-specific. This pattern indicates the importance of considering species' ballistics factors such as surface area and mass which affect drag when evaluating fall distributions (Prakash and Markfort, 2021). However, given that we saw an opposing effect of ground clearance on the fall distributions of two species with relatively small surface area and mass (Fig. 3d and e), it is evident there are other species-specific factors in play. Flight height and flight behavior may be some of these factors (Fig. 2).

The results of our model indicate that typical search plots in our dataset provided relatively good sampling of the hoary bat fall distribution (overlap between fit carcass density and proportion area searched: 0.837; Fig. 4a). In contrast, the fit carcass density for both horned larks and red-tailed hawks had comparatively less overlap with the proportion area searched (overlap of 0.447 and 0.529, respectively). This model result indicates that a substantial proportion of the horned lark and red-tailed hawk carcasses land in areas where <10 % of the area is searched (Fig. 4b and c). The qualitatively different flight behavioral strategies of these two species likely explains some of the differences in the shape of the fall distributions and perhaps their opposing relationship of ground clearance with fall distance. Horned larks tend to forage in large flocks below turbines (mean flight height of 19.9 m per Wulff et al., 2016; Fig. 2) whereas red-tailed hawks spend significant periods

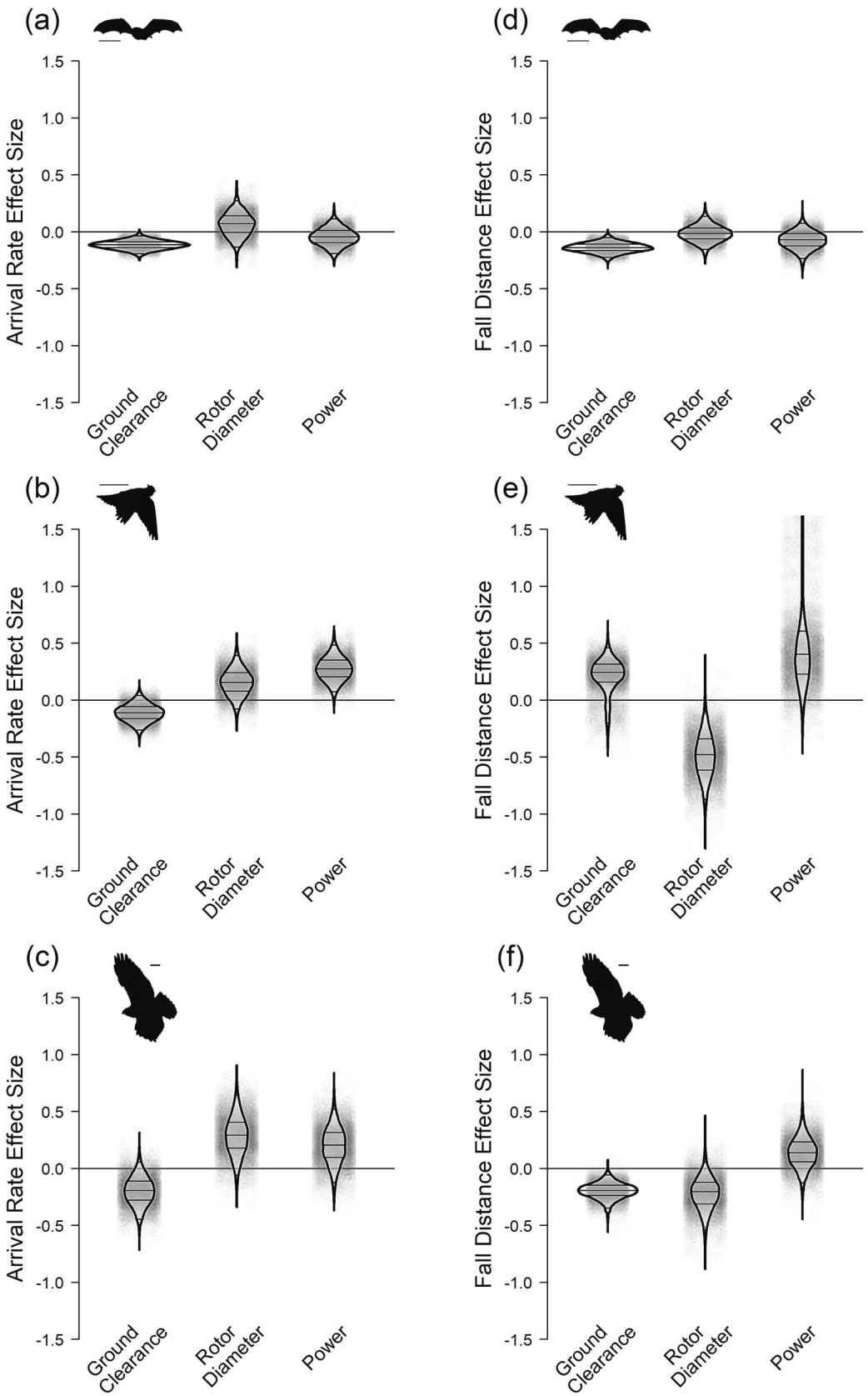

Fig. 3. Effect of selected turbine-size parameters on arrival (i.e., fatality) rates of (a) hoary bat, (b) horned lark, and (c) red-tailed hawk, as well as on fall distributions of (d) hoary bat, (e) horned lark, and (f) red-tailed hawk. Horizontal lines adjacent to silhouettes indicate relative scale of images.

Table 1
The four parameter types modeled for hoary bat, horned lark, and red-tailed hawk and the mean, standard deviation, and 95 % confidence intervals foreach parameter modeled per parameter type.

parameter type	Parameter	Hoary bat				Horned lark				Red-tailed hawk			
		Mean	SD	Lower 95 % CI	Upper 95 % CI	Mean	SD	Lower 95 % CI	Upper 95 % CI	Mean	SD	Lower 95 % CI	Upper 95 % CI
Arrival rate	log_ar_intercept	0.204	0.346	−0.467	0.819	−1.401	0.420	−2.238	−0.560	−3.180	0.439	−4.094	−2.352
	log_ar_ground_clearance	−0.115	0.039	−0.194	−0.039	−0.114	0.077	−0.266	0.037	−0.199	0.128	−0.451	0.049
	log_ar_rotor_diameter	0.062	0.106	−0.139	0.266	0.153	0.119	−0.084	0.384	0.285	0.176	−0.064	0.634
	log_ar_power	−0.045	0.078	−0.194	0.107	0.271	0.105	0.068	0.480	0.200	0.166	−0.133	0.521
	log_ar_region_error_sd	1.156	0.429	0.249	2.085	1.907	0.503	1.090	3.042	1.382	0.505	0.624	2.586
	log_ar_mosaic_error_sd	1.808	0.184	1.486	2.200	1.738	0.213	1.365	2.205	0.312	0.197	0.054	0.809
Fall distribution	log_fd_intercept	3.765	0.073	3.643	3.924	4.958	0.188	4.662	5.397	4.233	0.108	4.060	4.490
	log_fd_ground_clearance	−0.139	0.043	−0.226	−0.054	0.208	0.160	−0.209	0.450	−0.198	0.072	−0.352	−0.061
	log_fd_rotor_diameter	−0.018	0.073	−0.158	0.131	−0.492	0.200	−0.888	−0.108	−0.224	0.148	−0.542	0.052
	log_fd_power	−0.077	0.079	−0.239	0.073	0.491	0.440	−0.068	1.764	0.137	0.138	−0.137	0.418
	fd_sigma	0.933	0.065	0.823	1.074	0.709	0.070	0.583	0.858	0.458	0.094	0.310	0.685
	fd_df	4.319	0.671	3.362	5.867	3.572	0.523	2.709	4.759	2.596	0.788	1.715	4.379
Carcass persistence	logit_cp_intercept	2.077	0.258	1.581	2.577	1.632	0.179	1.268	1.982	2.763	0.163	2.441	3.084
	logit_cp_region_error_sd	0.678	0.215	0.240	1.147	0.583	0.142	0.355	0.908	0.416	0.200	0.012	0.811
	logit_cp_mosaic_error_sd	0.631	0.142	0.395	0.951	0.261	0.075	0.135	0.428	0.269	0.129	0.035	0.529
	logit_cp_season_error_sd	1.499	1.042	0.594	4.018	0.397	0.295	0.131	1.131	0.418	0.317	0.128	1.288
Searcher efficiency	logit_se_intercept	0.510	0.288	−0.032	1.060	0.421	0.187	0.034	0.791	1.277	0.217	0.857	1.708
	logit_se_region_error_sd	0.516	0.302	0.057	1.218	0.497	0.171	0.213	0.880	0.590	0.267	0.102	1.162
	logit_se_mosaic_error_sd	1.201	0.147	0.940	1.517	0.866	0.079	0.724	1.032	1.027	0.117	0.818	1.281
	logit_se_season_error_sd	1.402	0.942	0.519	3.867	0.517	0.364	0.166	1.490	1.098	0.842	0.289	3.415

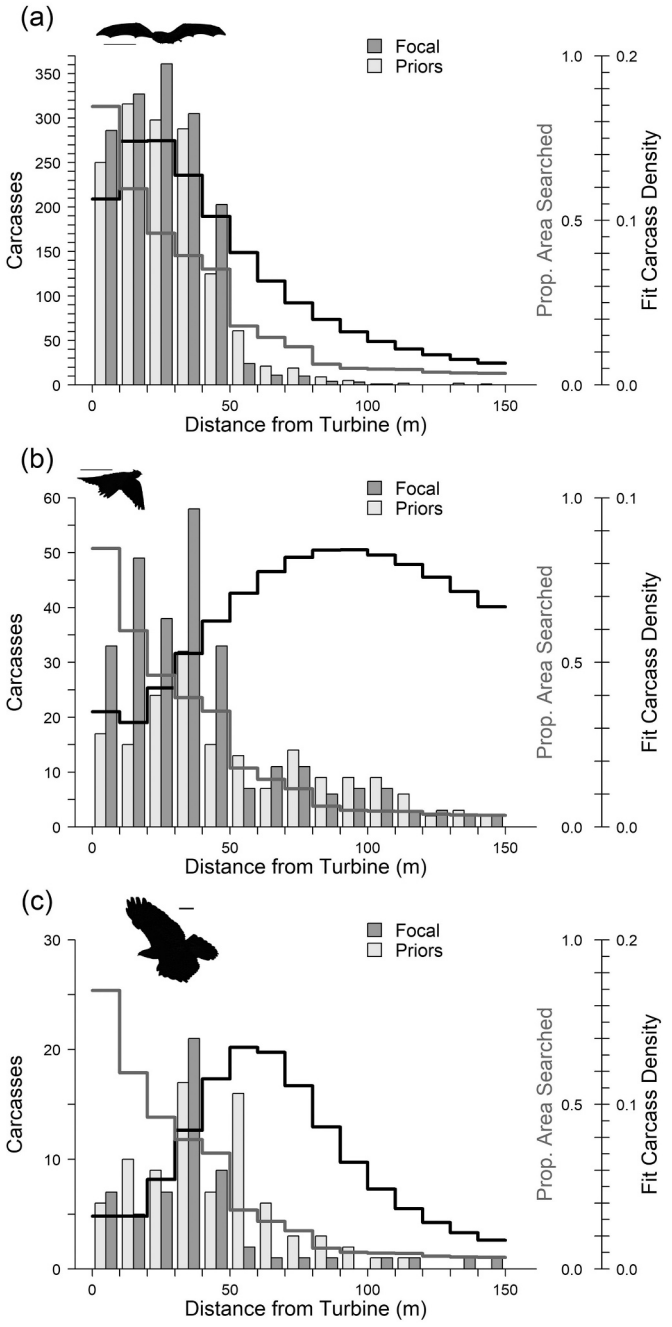

Fig. 4. Distribution of (a) hoary bat, (b) horned lark, and (c) red-tailed hawk carcasses detected relative to distance from turbine within the focal (dark grey) and priors (light grey) datasets. Fit carcass densities (black line) are shown along with the proportion of the area searched (grey line) per species. Horizontal lines adjacent to silhouettes indicate relative scale of images.

of time flying at or above the rotor-swept zone (mean flight height of 79.0 m per Wulff et al., 2016; Fig. 2). As demonstrated by Prakash and Markfort (2021), both the location of the collision on the blade as well as the position within the rotor plane affects the trajectory of carcasses and the distances thrown. For example, an object striking near the tip of a blade while it is sweeping through the bottom of the rotor-swept zone will fall differently than the same collision occurring while the blade is sweeping through the top of the rotor-swept zone.

As has been noted previously (Huso and Dalthorp, 2014), search plot size poses a key limitation on understanding the true fall distribution of species. Increasing the radius of a given search plot has significant cost consequences on the monitoring effort, and extrapolating fatality rates

for the area outside of the plot is fraught with largely uninformed assumptions, particularly since there are few empirical studies of carcass fall distributions (e.g., Hallingstad et al., 2018; Prakash and Markfort, 2021). Fatality estimates produced without appropriately accounting for species-specific fall distributions could lead to grossly mis-estimating actual mortality, and confound analyses into predictors of mortality. Thus, our findings underscore the importance of selecting the appropriate plot size and overall PCM study design for taxa of interest and research objectives, as well as the need for increased understanding of wildlife fall distributions.

4.3. Data biases and model implications

Qualitative structural differences between the two databases from which we derived our datasets heavily influenced our analysis. Systematic differences exist in sampling protocols between studies completed in Canada and studies completed in the U.S. (e.g., plot geometry, study seasons), many of which are influenced by regulatory requirements for PCM study design (e.g., Ontario Government, 2021) and affected the prioritization and types of the data collected. Under existing available fatality estimators (e.g., Dalthorp et al., 2017; Dalthorp et al., 2018) the considerable variation in sampling structure leads to either limiting analyses to complete datasets or backfilling data necessary for analysis. Our use of a Bayesian hierarchical model was necessary to facilitate information sharing among unevenly sampled and available data (Hobbs and Hooten, 2015). Furthermore, our use of a paired approach (i.e., mosaics) allowed us to isolate the effect of turbine size parameters within a given mosaic and compare relative differences in effects among mosaics.

4.4. Remaining research needs

Power rating is a crude proxy for actual power production and operational uptime, both of which likely influence wildlife fatality rates (Huso et al., 2021). Including actual power production data in future analyses of fatality rates and in wind fatality data repositories will better enable the wind energy industry to minimize wildlife impacts while maximizing energy production, such as through smart curtailment strategies. Whereas our research investigated the effect of absolute turbine size, we did not assess the effect of turbine density within our mosaics. Often, a reduction in installed turbine density is a byproduct of increased power generation with larger turbines, for both greenfield and repowers that involve full turbine replacements. The interaction between turbine density and turbine size on wildlife impacts is one meriting further research.

CRediT authorship contribution statement

Julie C. Garvin: Conceptualization, Data curation, Funding acquisition, Investigation, Methodology, Writing – original draft, Writing – review & editing. **Juniper L. Simonis:** Conceptualization, Data curation, Formal analysis, Methodology, Software, Validation, Writing – original draft, Writing – review & editing. **Jennifer L. Taylor:** Data curation, Funding acquisition, Investigation, Methodology, Project administration, Writing – original draft, Writing – review & editing.

Declaration of competing interest

Julie Garvin reports financial support was provided by Renewable Energy Wildlife Research Fund (grant number BE-01). This research was initiated, funded and conducted while J.G. was primarily employed by Tetra Tech. Prior to completion of this manuscript, J.G. accepted employment at a company that is a member of REWRF. This company did not provide funding for this study and neither did it review the study design or reports, including this manuscript. J.G. was retained on an on-call basis by Tetra Tech explicitly for the purposes of completing this research.

Data availability

Public data (S1) and code (S3) used are available in supplemental materials; a detailed data availability statement indicates how to request access to 3rd party confidential data repositories.

Acknowledgements

The authors thank Taber Allison and Ryan Butryn of the Renewable Energy Wildlife Institute for curating PCM data from the AWWIC database for analysis as well as input on this manuscript. Thanks also go to Catherine Jardine of Birds Canada for curating and contributing PCM data from the WEBBMD, and to the industry proponents (and individuals or consultants working on their behalf) who contributed data to both databases, and to our study directly. In addition to the research grant mentioned above, funding was also provided through in-kind donations from DAPPER Stats, and Tetra Tech, Inc.

Appendix A. Supplementary data

Supplementary data to this article can be found online at Appendix S1 Priors (Reference data) (Mendeley Data); Appendix S2 Data Selection and Adjustments; Appendix S3 Code, Priors Dataset, Results (Original data) (Mendeley Data).

References

Anderson, A.M., Jardine, C.B., Zimmerling, J.R., Baerwald, E.F., Davy, C.M., 2022. Effects of turbine height and cut-in speed on bat and swallow fatalities at wind energy facilities. Facets 7, 1281–1297. https://doi.org/10.1139/facets-2022-0105.

Arnett, E.B., Baerwald, E.F., 2013. Impacts of wind energy development on bats: implications for conservation. In: Adams, R.A., Pedersen, S.C. (Eds.), Bat Ecology, Evolution and Conservation. eSpringer Science Press, New York, pp. 435–456. https://doi.org/10.1007/978-1-4614-7397-8_21.

Arnett, E.B., Brown, W.K., Erickson, W.P., Fiedler, J.K., Hamilton, B.L., Henry, T.H., Jain, A., Johnson, G.D., Kerns, J., Koford, R.R., Nicholson, C.P., O'Connell, T.J., Piorkowski, M.D., Tankersley, R.D., 2008. Patterns of bat fatalities at wind energy facilities in North America. J. Wildl. Manag. 72, 61–78. https://doi.org/10.2193/2007-221.

AWWI, 2020a. AWWI Technical Report: 2nd Edition: Summary of Bird Fatality Monitoring Data Contained in AWWIC. Washington, DC. Available at. http://www.awwi.org.

AWWI, 2020b. AWWI Technical Report: 2nd Edition: Summary of Bat Fatality Monitoring Data Contained in AWWIC. Washington, DC. Available at. http://www.awwi.org.

AWWI (American Wind Wildlife Institute), 2017. Wind Turbine Interactions with Wildlife and their Habitats – A Summary of Research Results and Priority Questions. American Wind Wildlife Institute, Washington, DC. https://awwi.org/wp-content/uploads/2017/07/AWWI-Wind-Wildlife-Interactions-Summary_Literature-Cited-June-2017.pdf.

Baerwald, E.F., Edworthy, J., Holder, M., Barclay, R.M.R., 2009. A large-scale mitigation experiment to reduce bat fatalities at wind energy facilities. J. Wildl. Manag. 73, 1077–1081. https://doi.org/10.2193/2008-233.

Band, W., Madders, M., Whitfield, D.P., 2007. Developing field and analytical methods to assess avian collision risk at wind farms. In: de Lucas, M., Janss, G.F.E., Ferrer, M. (Eds.), Birds and Windfarms: Risk Assessment and Mitigation. Quercus, Madrid, pp. 259–275 (ISBN: 9788487610189).

Barclay, R.M.R., Baerwald, E.F., Gruver, J.C., 2007. Variation in bat and bird fatalities at wind energy facilities: assessing the effects of rotor size and tower height. Can. J. Zool. 85, 381–387. https://doi.org/10.1139/Z07-011.

Bird Studies Canada, NABCI (North American Bird Conservation Initiatives), 2014. Bird Conservation Regions. Published by Bird Studies Canada on behalf of the North American Bird Conservation Initiative. https://www.birdscanada.org/bird-science/nabci-bird-conservation-regions. (Accessed 13 August 2021).

Chandler, R.B., Royle, J.A., King, D.I., 2011. Inference about density and temporary emigration in unmarked populations. Ecology 92 (7), 1429–1435. https://doi.org/10.1890/10-2433.1 (Erratum in: Ecology. 95(3), 794. PMID: 21870617).

Cooch, E., White, G., 2002. Program MARK: A Gentle Introduction. Colorado State University, Colorado.

Cryan, P.M., Gorresen, P.M., Hein, C.D., Schirmacher, M.R., Diehl, R.H., Huso, M.M., Hayman, D.T.S., Fricker, P.D., Bonaccorso, F.J., Johnson, D.H., 2014. Behavior of bats at wind turbines. Proc. Natl. Acad. Sci. 111, 15126–15131. https://doi.org/10.1073/pnas.1406672111.

Dail, D., Madsen, L., 2011. Models for estimating abundance from repeated counts of an open metapopulation. Biometrics 67, 577–587. https://doi.org/10.1111/j.1541-0420.2010.01465.x.

Dalthorp, D., Huso, M., Dail, D., 2017. Evidence of Absence (v2.0) Software User Guide: U.S. Geological Survey Data Series 1055. https://doi.org/10.3133/ds1055.

Dalthorp, D., Simonis, J., Madsen, L., Huso, M., Rabie, P., Mintz, J.M., Wolpert, R., Studyvin, J., Korner-Nievergelt, F., 2018. Generalized Mortality Estimator (GenEst) - R Code & GUI: U.S. Geological Survey Software Release. https://doi.org/10.5066/P9O9BATL.

de Lucas, M., Janss, G.F.E., Whitfield, D.P., Ferrer, M., 2008. Collision fatality of raptors in wind farms does not depend on raptor abundance. J. Appl. Ecol. 45, 1695–1703. https://doi.org/10.1111/j.1365-2664.2008.01549.x.

de Valpine, P., Turek, D., Paciorek, C.J., Anderson-Bergman, C., Temple Lang, D., Bodik, R., 2017. Programming with models: writing statistical algorithms for general model structures with NIMBLE. J. Comput. Graph. Stat. 26, 403–413. https://doi.org/10.1080/10618600.2016.1172487.

de Valpine, P., Paciorek, C., Turek, D., Michaud, N., Anderson-Bergman, C., Obermeyer, F., Wehrhahn Cortes, C., Rodrìguez, A., Temple Lang, D., Paganin, S., . NIMBLE: MCMC, Particle Filtering, and Programmable Hierarchical Modeling. R package version 0.12.2. https://cran.r-project.org/package=nimble. https://doi.org/10.5281/zenodo.1211190.

EPRI (Electric Power Research Institute), 2020. Population-level risk to hoary bats amid continued wind energy development: assessing fatality reduction targets under broad uncertainty. In: Technical Report No. 300201761. Palo Alto, CA. https://www.epri.com/research/products/000000003002017671.

Erickson, W.P., Wolfe, M.M., Bay, K.J., Johnson, D.H., Gehring, J.L., 2014. A comprehensive analysis of small-passerine fatalities from collision with turbines at wind energy facilities. PloS One 9, e107491 (http://dx.doi.org/10.1371%2Fjournal.pone.0107491).

Everaert, J., 2014. Collision risk and micro-avoidance rates of birds with wind turbines in Flanders. Bird Study 61, 220–230. https://doi.org/10.1080/00063657.2014.894492.

Fiedler, J.K., Henry, T.H., Tankersley, R.D., Nicholson, C.P., 2007. Results of Bat and Bird Mortality Monitoring at the Expanded Buffalo Mountain Windfarm, 2005. Tennessee Valley Authority (June 28, 2007).

Foo, C.F., Bennett, V.J., Hale, A.M., Korstian, J.M., Schildt, A.J., Williams, D.A., 2017. Increasing evidence that bats actively forage at wind turbines. PeerJ 5, e3985. https://doi.org/10.7717/peerj.3985.

Friedenberg, N.A., Frick, W.F., 2021. Assessing fatality minimization for hoary bats amid continued wind energy development. Biol. Conserv. 262, 109309 https://doi.org/10.1016/j.biocon.2021.109309.

Gelman, A., Rubin, D.B., 1992. Inference from iterative simulation using multiple sequences. Stat. Sci. 7, 457–511. https://www.jstor.org/stable/2246093.

Gelman, A., Carlin, J.B., Stern, H.S., Rubin, D.B., 2014. Bayesian Data Analysis, third ed. CRC Press, Florida (ISBN 9781439840955).

Goldstein, B., Turek, D., Ponisio, L., de Valpine, P., 2021. nimbleEcology: Distributions for Ecological Models in nimble. R package version 0.4.1. https://cran.r-project.org/package=nimbleEcology.

Haines, L.M., 2016. Maximum likelihood estimation for N-mixture models. Biometrics 72, 1235–1245. https://doi.org/10.1111/biom.12521.

Haines, L.M., 2020. Multinomial N-mixture models for removal sampling. Biometrics 76, 540–548. https://doi.org/10.1111/biom.13147.

Hallingstad, E.C., Rabie, P.A., Telander, A.C., Roppe, J.A., Nagy, L.R., 2018. Developing an efficient protocol for monitoring eagle fatalities at wind energy facilities. PloS One 13 (12), e0208700. https://doi.org/10.1371/journal.pone.0208700.

Hobbs, N.T., Hooten, M.B., 2015. Bayesian Models: A Statistical Primer for Ecologists. Princeton University Press, New Jersey (ISBN 9780691159287).

Hull, C.L., Muir, S., 2010. Search areas for monitoring bird and bat carcasses at wind farms using a Monte-Carlo model. Australasian J. Environ. Manag. 17, 77–87. https://doi.org/10.1080/14486563.2010.9725253.

Huso, M., Dalthorp, D., 2014. Accounting for unsearched areas in estimating wind turbine-caused fatality. J. Wildl. Manag. 78, 347–358. https://doi.org/10.1002/jwmg.663.

Huso, M., Conkling, T., Dalthorp, D., Davis, M., Smith, H., Fesnock, A., Katzner, T., 2021. Relative energy production determines effect of repowering on wildlife mortality at wind energy facilities. J. Appl. Ecol. 00, 1–7. https://doi.org/10.1111/1365-2664.13853.

Khosravifard, S., Skidmore, A.K., Naimi, B., Venus, V., Muñoz, A.R., Toxopeus, A.G., 2020. Identifying birds' collision risk with wind turbines using a multidimensional utilization distribution method. Wildl. Soc. Bull. 44, 191–199. https://doi.org/10.1002/wsb.1056.

Krijgsveld, K.L., Akershoek, K., Schenk, F., Dijk, F., Dirksen, S., 2009. Collision risk of birds with modern large wind turbines. Ardea 97 (3), 357–366. https://doi.org/10.5253/078.097.0311.

Kruschke, J.K., 2015. Doing Bayesian Data Analysis: A Tutorial with R, JAGS, and Stan. Academic Press, California (ISBN 978-0-12-405888-0).

Lacal-Arántegui, R., Uihlein, A., Yusta, J.M., 2020. Technology effects in repowering wind turbines. Wind Energy 23, 660–675. https://doi.org/10.1002/we.2450.

LaNier, M.W., 2005. LWST Phase I project conceptual design study: evaluation of design and construction approaches for economical hybrid steel/concrete wind turbine towers June 28, 2002 – July 31, 2004. In: National Renewable Energy Laboratory Report SR-500-36777. http://www.osti.gov/bridge.

Lantz, E., Roberts, O., Nunemaker, J., DeMeo, E., Dykes, K., Scott, G., 2019. Increasing Wind Turbine Tower Heights: Opportunities and Challenges. National Renewable Energy Laboratory, Colorado. NREL/TP-5000-73629. https://www.nrel.gov/docs/fy19osti/73629.pdf.

Loss, S.R., Will, T., Marra, P.P., 2013. Estimates of bird collision mortality at wind facilities in the contiguous United States. Biol. Conserv. 168, 201–209. https://doi.org/10.1016/j.biocon.2013.10.007.

Marques, A.T., Batalha, H., Rodrigues, S., Costa, H., Pereira, M.J.R., Fonseca, C., Mascarenhas, M., Bernardino, J., 2014. Understanding bird collisions at wind farms: an updated review on the causes and possible mitigation strategies. Biol. Conserv. 179, 40–52. https://doi.org/10.1016/j.biocon.2014.08.017.

Marriot, N., 2022. tmux. v 3.3a. June 9, 2022. https://github.com/tmux/tmux.

Maurer, J.D., Huso, M., Dalthorp, D., Madsen, L., Fuentes, C., 2020. Comparing methods to estimate the proportion of turbine-induced bird and bat mortality in the search area under a road and pad search protocol. Environ. Ecol. Stat. 27, 769–801. https://doi.org/10.1007/s10651-020-00466-0.

Menzel, J.M., Menzel, M.A., Kilgo, J.C., Ford, W.M., Edwards, J.W., McCracken, G.F., 2005. Effect of habitat and foraging height on bat activity in the coastal plain of South Carolina. J. Wildlife Manag. 69, 235–245. https://doi.org/10.2193/0022-541X(2005)069<0235:EOHAFH>2.0.CO;2. Medium: ED; Size.

Minderman, J., Fuentes-Montemayor, E., Pearce-Higgins, J.W., Pendlebury, C.J., Park, K. J., 2015. Estimates and correlates of bird and bat mortality at small wind turbine sites. Biodivers. Conserv. 24, 467–482. https://doi.org/10.1007/s10531-014-0826-z.

Nicholson, J.C., 2011. Design of Wind Turbine Tower and Foundation Systems: Optimization Approach. Master's Thesis. University of Iowa. https://doi.org/10.17077/etd.bhnu76gr.

Ontario Government, 2021. Regulation 359/09 of the Environmental Protection Act 2019. https://www.ontario.ca/page/bats-and-bat-habitats-guidelines-wind-power-projects#section-5.

Peterson, T., Byrne, C., Rusk, A., 2022. EchoPitch: using acoustics to measure and manage risk to bats at commercial wind energy facilities. In: Presentation at the 14th Wind Wildlife Research Meeting, November 14–17, 2022. Kansas City, Missouri.

Plard, F., Turek, D., Grüebler, M.U., Schaub, M., 2019. IPM2: toward better understanding and forecasting of population dynamics. Ecol. Monogr. 89 (3), e01364 https://doi.org/10.1002/ecm.1364.

Plummer, M., Best, N., Cowles, K., Vines, K., 2006. CODA: convergence diagnosis and output analysis for MCMC. R News 6, 7–11. http://cran.r-project.org/doc/Rnews/Rnews_2006-1.pdf#page=7.

Prakash, S., Markfort, C.D., 2021. Experimental investigation of aerodynamic characteristics of bat carcasses after collision with a wind turbine. Wind Energ. Sci. 5, 745–758. https://wes.copernicus.org/articles/5/745/2020/.

R Core Team, 2022. R: A Language and Environment for Statistical Computing. R Foundation for Statistical Computing, Austria. https://www.R-project.org/.

Roeleke, M., Blohm, T., Kramer-Schadt, S., Yovel, Y., Voigt, C.C., 2016. Habitat use of bats in relation to wind turbines revealed by GPS tracking. Sci. Rep. 6, 28961. https://doi.org/10.1038/srep28961.

Royle, J.A., 2004. Generalized estimators of avian abundance from count survey data. Anim. Biodivers. Conserv. 27 (1), 375–386 (e-ISSN: 2014-928X).

Sassi, M.A., 2016. Nonlinear Dynamic Analysis of Wind Turbine Towers Subject to Design Wind and Seismic Loads (Ph.D. Dissertation). Colorado School of Mines. http://hdl.handle.net/11124/170630.

Schaub, M., Abadi, F., 2011. Integrated population models: a novel analysis framework for deeper insights into population dynamics. J. Ornithol. 152, S227–S237. https://doi.org/10.1007/s10336-010-0632-7.

Shaby, B., Wells, M., 2011. Exploring an Adaptive Metropolis Algorithm. Technical Report 2011-14. Department of Statistics, Duke University.

Smales, I., Muir, S., Meredith, C., Baird, R., 2013. A description of the biosis model to assess risk of bird collisions with wind turbines. Wildl. Soc. Bull. 37, 59–65. https://doi.org/10.1002/wsb.257.

Smallwood, K.S., 2013. Comparing bird and bat fatality-rate estimates among North American wind-energy projects. Wildl. Soc. Bull. 37 (1), 19–33. https://doi.org/10.1002/wsb.260.

Sollmann, R., Gardner, B., Chandler, R.B., Royle, J.A., Sillett, T.S., 2015. An open-population hierarchical distance sampling model. Ecology 96, 325–331. https://doi.org/10.1890/14-1625.1.

Sólymos, P.S., Lele, S., Bayne, E., 2012. Conditional likelihood approach for analyzing single visit abundance survey data in the presence of zero inflation and detection error. Environmetrics 23, 197–205. https://doi.org/10.1002/env.1149.

Thompson, M., Beston, J.A., Etterson, M., Diffendorfer, J.E., Loss, S.R., 2017. Factors associated with bat mortality at wind energy facilities in the United States. Biol. Conserv. 215, 241–245. https://doi.org/10.1016/j.biocon.2017.09.014.

Tucker, V.A., 1996. Using a collision model to design safer wind turbine rotors for birds. J. Solar Energy Eng.-Trans. Am. Soc. Mech. Eng. 118, 263–269. https://doi.org/10.1115/1.2871791.

U.S. Department of Energy, 2019. 2019 Wind Energy Data & Technology Trends. Wind Technologies Office, Office of Energy Efficiency & Renewable Energy. https://www.energy.gov/eere/wind/2019-wind-energy-data-technology-trends#wind (accessed August 21, 2021).

Watson, R., Kolar, P., Ferrer, M., Nygård, T., Johnston, N., Hunt, W.G., Smit-Robinson, H., Farmer, C., Huso, M., Katzner, T., 2018. Raptor interactions with wind energy: case studies from around the world. J. Raptor Res. 52 (1), 1–18. https://doi.org/10.3356/JRR-16-100.1.

Wind Energy Bird and Bat Monitoring Database (WEBBMD). Data Accessed From Bird Studies Canada. http://www.naturecounts.ca/birdmon/wind. (Accessed 11 December 2020).

Wulff, S.J., Butler, M.J., Ballard, W.B., 2016. Assessment of diurnal wind turbine collision risk for grassland birds on the southern Great Plains. J. Fish Wildl. Manag. 7 (1), 129–140. https://doi.org/10.3996/042015-JFWM-031.

Wyatt, R.J., 2002. Estimating riverine fish population size from single- and multiple-pass removal sampling using a hierarchical model. Can. J. Fish Aquat. Sci. 59, 695–706. https://doi.org/10.1139/f02-041.

Zimmerling, J.R., Francis, C.M., 2016. Bat mortality due to wind turbines in Canada. J. Wildl. Manag. 80, 1360–1369. https://doi.org/10.1002/jwmg.21128.

Zipkin, E.F., Sillett, T.S., Grant, E.H.C., Chandler, R.B., Royle, J.A., 2014. Inferences about population dynamics from count data using multistate models: a comparison to capture–recapture approaches. Ecol. Evol. 4 (4), 417–426. https://onlinelibrary.wiley.com/doi/full/10.1002/ece3.942.